

# TWO KILOWATT BIROPELLANT ARCJET DEVELOPMENTS

KURT HOHMAN, THOMAS BROGAN, & VLADIMIR HRUBY  
BUSEK COMPANY, INC., 11 TECH CIRCLE, NATICK, MA 01760, USA

KURT ANNEN & ROBERT BROWN  
AERODYNE RESEARCH, INC., 45 MANNING ROAD, BILLERICA, MA 01821

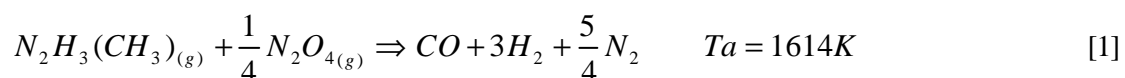
## Introduction

Since the Gemini, Apollo, Viking Orbiter, et al. missions launched in 1960's and 1970's, bipropellant chemical thrusters have dominated spacecraft propulsion. In particular, Monomethylhydrazine (MMH) plus Nitrogen Tetroxide (NTO) and to a lesser extent Unsymmetrical Dimethylhydrazine (UDMH) are by far the most widely utilized rocket propellants for apogee insertion and reaction control. As a result, a vast array of devices, infrastructure and experience has been accumulated, which will continue to be used in the foreseeable future. However, attitude control system and station keeping functions are increasingly performed by electric propulsion (EP). Ideal for this purpose would be an EP device that uses the same bipropellant and associated feed system components that are already on-board and continue to take advantage of the aforementioned experience and infrastructure. An arcjet fueled by conventional bipropellants would fulfill this role, increasing the mission average specific impulse ( $I_{sp}$ ), lowering the propulsion system wet mass and spacecraft launch costs. The bipropellant arcjet can achieve high thrust and high efficiency by combining chemical energy with electrical power.

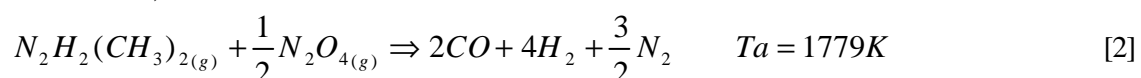
Development of an arcjet that is fueled by carbon containing propellants began at Busek in the mid 1990's. A unique methane arcjet was developed.<sup>1</sup> This program proved an arcjet could operate under these conditions, however, the plume contained carbon particles – a potential contaminate of the spacecraft. Following this program, Busek conceived the idea of oxidizing the carbon into CO before passing through the arc, knowing that CO is very stable. Using methanol ( $CH_3OH$ ) as the fuel, Busek proved through arcjet experiments that if all the carbon is oxidized to CO, no internal carbon deposition takes place, no carbon particles exist in the plume, and no corrosion of the arcjet construction material occurs. This led to the present work on the bipropellant arcjet fueled by a mixture of MMH (or UDMH) with NTO in proportions that generate CO, leaving no free oxygen or carbon. The experiments and numerical simulations proved the chemical kinetics of reforming to be too slow for application in a typical DC arcjet. This led to the development of an RF arcjet fueled by approximately stoichiometric mixture of simulated MMH/NTO. The effort was very successful and validated the feasibility of this type of thruster with a variety of reactants and proved that superimposing electrical energy addition on chemical energy addition to achieve high performance rocket is viable.

## DC Bipropellant Arcjet Development – Reforming Mode

The goal of this project was to reform MMH with appropriate amounts of NTO to form carbon monoxide (CO) without any further carbon or oxygen remaining, followed by passing the gas products through a typical arcjet for unique performance. The resulting CO molecule is extremely stable and does not precipitate carbon when heated. In addition, CO is non-corrosive against tungsten and other materials of construction for arcjets. This reforming must take place within the arcjet combustion chamber, but before the arc, in order to take advantage of the chemical energy release plus prevent the carbon/oxidizing problems. If the reforming were to take place external to the arcjet, similar to the catalytic decomposition of hydrazine ( $N_2H_4$ ), carbon would condense onto the catalyst at these fuel/oxidizer ratios, reducing the functionality of the catalyst and possibly plugging it with carbon. The reforming reaction between MMH & NTO to form CO is given by:



and for UDMH and NTO,



The reforming reaction for hydrazine is given by:



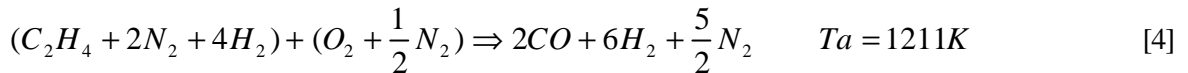
Here,  $T_a$  is the adiabatic reaction temperature for the respective reforming reaction.

Note that the oxidizer required to reform the propellants to  $N_2$ ,  $H_2$  and  $CO$  is 20% and 25% for MMH and UDMH respectively of the amount required to fully oxidize the propellants to carbon dioxide and water vapor.

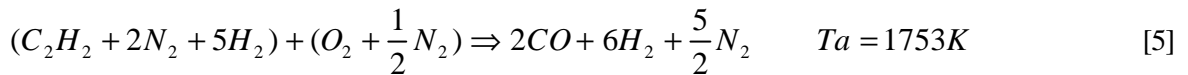
### Simulation of MMH/NTO in the Laboratory

Busek's laboratory is not equipped to handle the actual MMH or UDMH propellants. Therefore, they were simulated using gas mixtures of hydrogen, nitrogen and acetylene or ethylene. NTO was simulated with a gas mixture of oxygen and nitrogen. The MMH and UDMH molecules have positive heats of formation of 22.5 and 20.2 kcal/gm-mole respectively in the liquid phase. The high heats of formation of MMH and UDMH, together with the energy released in partial combustion to  $CO$ , account for the relatively high adiabatic reforming temperatures of 1614K and 1779K respectively. Since we only simulated MMH in the laboratory and UDMH would perform similarly, UDMH will not be discussed in great detail for the remainder of this paper.

We considered two gaseous hydrocarbons to simulate MMH; ethylene and acetylene. The gas mixtures and the reaction to simulate MMH + NTO with ethylene mixture are:



While for MMH + NTO simulated with acetylene mixture, the reaction is:



The adiabatic reforming temperature for the ethylene mixture is 1211K versus 1614K for the real propellant (MMH) and for the acetylene mixture the reforming temperature is 1753K, which is slightly higher than MMH. It was anticipated that the higher reforming temperature would prove essential for complete reforming, therefore, acetylene was baselined for initial experiments. Unfortunately, acetylene is unstable at pressures above 20psig and may spontaneously decompose. With arc chamber pressures of 50 psig or more, it is not possible to inject acetylene directly into gas mixing manifolds at these pressures. Therefore, initial experiments utilized the ethylene mixtures until we could design and construct an acetylene-hydrogen-nitrogen gas compression system explained next.

One solution to the acetylene stability problem is to mix at low pressure, ~15 psig, the acetylene with hydrogen and nitrogen in proper ratios to simulate MMH, and then compress the mixture to high pressures making sure the acetylene partial pressure never exceeds 30 psia. A gas-compression system with autonomous programmable controller was designed to allow for acetylene containing gas mixtures to be compressed well above the arc chamber pressure (~50psig). Using a small air compressor, the intake was connected to a gas mixing manifold fed by three ratio-controlled, calibrated MKS mass flow controllers. The molar ratios are given by  $(C_2H_2 + 2N_2 + 5H_2)$  and the acetylene partial pressure is by definition  $P_{C_2H_2} = (1 \text{ mol } C_2H_2 / 8 \text{ mol total}) \times P_{\text{total}}$ . Therefore, the maximum  $P_{\text{total}}$  is 240 psia to safely compress acetylene at  $P_{C_2H_2} \leq 30$  psia. Since 240 psia injection pressure is not needed, we set the maximum compression pressure to 134.7 psia, for a safety factor of 1.8. In addition, several flow and pressure interlocks were installed in case one of the input gases flows were reduced or the compressor malfunctioned.

### Estimated Vacuum Performance of Reformed MMH and UDMH

The approximate relative performance of internally reformed MMH and UDMH compared to hydrazine can be calculated with simplifying assumptions. The similarity of the carbon monoxide and nitrogen molecules means the discharge in the reformed mixtures should be similar to that of reformed hydrazine with the exception of the effect of the different  $H_2/(CO + N_2)$  ratios on frozen expansion efficiency and  $I_{sp}$ , and the influence of internal reforming on overall efficiency.

The estimated frozen flow, vacuum specific impulse ( $I_{spv}$ ) and frozen flow, vacuum expansion efficiency,  $f$  (the fraction of total energy supplied to the propellant, chemical plus electrical, that is converted to kinetic energy), of MMH and UDMH reformed with  $N_2O_4$  has been computed and compared with that of reformed  $N_2H_4$ . Figure 1 compares the  $I_{spv}$  versus mean arc chamber temperature for the three propellants under the assumptions: 1) Hydrogen dissociation equilibrium in the arc chamber and frozen during the expansion, 2)  $N_2$  and  $CO$  are not dissociated. The second assumption is valid to about 6000 K, above which the very large dissociation energy of  $CO$  and  $N_2$  acts as an effective brake to higher  $I_p$  with propellants containing these molecules. Clearly, hydrazine is the propellant of choice when maximum  $I_{sp}$  is the governing criterion while UDMH is the choice to maximize efficiency.

State of the art hydrazine arcjet thrusters exhibit an actual  $I_{sp}$  of about 600 seconds. The vacuum  $I_{spv}$  is probably around 650 seconds. On this basis, similar thrusters operating on MMH and UDMH may be expected to have actual  $I_{sp}$  of around 535 and 515 seconds respectively on the basis of the data presented in Figure 1.

For what type of mission would the use of MMH or UDMH internally reformed with  $N_2O_4$  be attractive? First of all, for those systems where these propellants and  $N_2O_4$  form a primary chemical propulsion system and their use would make it unnecessary to carry a third propellant. These systems would probably include those where the total velocity increment for the electric propulsion portion of the mission is modest. Second, are systems that are power limited, but short of thrust with which to execute rapid maneuvers and requiring  $I_{sp}$  substantially above that achievable by purely chemical thrusters. It was chosen to center the size of the arcjet around 2kW as this power level was thought to give the bipropellant the highest number of satellite mission opportunities. At 2 kW, assumed  $I_{spv}$  of 575s and electric to kinetic energy conversion efficiency ( $\eta$ ) including frozen losses of 40%, and the arcjet mass flow ( $\dot{m}$ ) defined as:

$$\dot{m} = \frac{2Ph}{(I_{sp} g_o)^2} \quad [6]$$

yields  $\dot{m} = 0.05$  gm/s. The volumetric flow rate is 5slpm (1340 ACFM) at 0.1Torr vacuum tank pressure. If the arc should extinguish, 1 mole of  $O_2$  will be unreacted and since we are also injecting  $H_2$ , for combustion limits the partial pressure of  $O_2$  must remain below 5% for partial pressures of  $H_2$  of 10% or greater. We chose to dilute the vacuum tank with  $N_2$  in order to keep  $O_2$  partial pressure below 5%. For an arc gas flow of 5slpm, the dilution flow of  $N_2$  needs to be 5.5slpm (10.5mol/9.5mol) x (5slpm) minimum, assuming no air leaks. Therefore, total volumetric flow is 10.5slpm or 2814 ACFM at 0.1Torr. Of course the desire to operate at slightly higher flows and lower tank pressures is likely and we sized our facility pumping capacity appropriately.

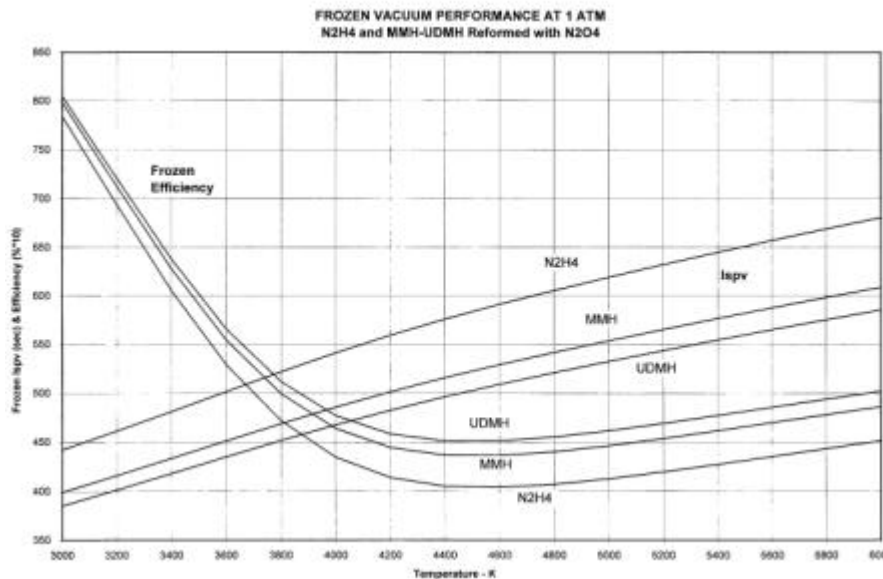


**Figure 1 Estimated  $I_{spv}$  and Frozen Flow Efficiency for  $N_2H_4$ , and Reformed MMH and UDMH as a function of Arc Mean Temperature.**

### Arcjet Facility

The arcjet test facility is pictured in Figure 2 and Figure 3. The stainless steel vacuum test chamber is six feet in diameter by eight feet in length. The pumping system is a three pump series consisting of two mechanical Roots style blowers and one rotary-piston oil mechanical pump. The vacuum side blower is a Roots 1024 RGS-HVB with 5200 ACFM pumping capacity at pressures of 0.1Torr and an ultimate vacuum of  $\sim 1 \times 10^{-4}$  Torr. The intermediate blower is a Roots 612 RGS-HVB with 1400 ACFM pumping capacity at pressure of 1 Torr. The roughing pump is a Leybold built NRC 200S with 200 CFM pumping capacity. A significant portion of the initial arcjet testing was performed in a smaller, 3 foot diameter tank with only the 615 RGS and NRC 200S pumps before the facility was upgraded. The mass flow controllers are MKS type 1179 with model 247 4 channel readouts. The flow controls and acetylene mixture compression cabinets are pictured in the left-hand side of Figure 3. The arcjet power supply is a Halmar Robicon 20kW HR1000

switching (1kHz) power supply rated at 125V 160A and is equipped with a customized DC 12mH line reactor in series with the load. A conventional welding high frequency starter (Miller HF-250D-1) provided arc starting. In addition, a natural gas fueled gas burner was installed in vacuum pump exhaust line to burn off any non-reacted combustibles or toxic products.



**Figure 2 Busek's arcjet facility showing pumping system.**



**Figure 3 Front view of arcjet facility & control cabinets.**

### DC Bipropellant Arcjet Experiments

Preliminary tests were performed with a water-cooled arcjet as a guide for the initial arcjet design and scaling in order to conserve limited financial resources. A commercial thermal spray gun was purchased, Tyrolit PG-100-4, and the housing, power, water and gas connections were utilized. This gave us an restricted anode and cathode interior design and fabrication as long as they fit within the dimensions of this housing. Copper nozzle blanks (solid preforms, only interior needs machining) and 2% thoriated tungsten cathodes were readily available from the manufacturer. A typical copper anode/nozzle and 2% thoriated tungsten cathode are sketched in Figure 4. All tests utilized gas mixture of (19%CO + 24%N<sub>2</sub> + 57%H<sub>2</sub>) simulating the reformed products of MMH and nitrogen tetroxide. Operating a water-cooled arcjet with the reforming mixture (C<sub>2</sub>H<sub>2</sub> + 2N<sub>2</sub> + 5H<sub>2</sub> + O<sub>2</sub> + ½ N<sub>2</sub>), would condense carbon precipitates out of the combusting gas. A condensed listing of the test results is given in Table 1 and a sample plume of the arcjet is pictured in Figure 5.

After a first attempt to operate the arcjet with a 2.03mm throat (constrictor) diameter and a 20° included angle of convergence were unable to obtain a stable arc, a second anode with 2.03mm diameter throat and 90° included angle of convergence was fabricated. This configuration was stable and the range of results are given in Table 1, row one. A plurality of cathode to anode gaps were from 1.52mm to 2.79mm. The highest electrical to thermal efficiency (71%) was obtained with a flow of 15 slpm and power of 6kW, and these results were used for scaling purposes.

For a 2kW MMH/NTO arcjet with an I<sub>sp</sub> of 520s, overall efficiency of η=40%, the volumetric flow rate is 6slpm. Therefore, the flow scaling between 15slpm/6slpm is 2.5 which yields a throat diameter of 1.27mm. Those results are given in Table 1, row 2. All runs with this geometry exhibited throat diameter enlargement with time. The copper throat has shown evidence of melting due to insufficient water cooling.

**Table 1 Water-cooled arcjet test results, gas feed (19%CO + 24%N<sub>2</sub> + 57%H<sub>2</sub>).**

Throat Dia. (mm)	Power (kW)	Gas Flow (slpm) (g m/s)	Specific Power (kJ/gm)	Efficiency (electric-thermal)
2.03	4.0-6.8	(10-20) (0.098-0.196)	33-43	67-71%
1.27	2.0-3.5	(5-12) (0.049-0.117)	29-46	29-60%

The next most practical step in the bipropellant arcjet evolution was a hybrid arcjet. We define the hybrid arcjet as a radiation-cooled combustion chamber, constrictor and nozzle attached to a water-cooled power connector block as sketched in Figure 6 and a picture of one configuration is displayed in Figure 7. The gas injectors may also be attached to the water-cooled block, but in most cases they were connected to the radiation cooled section. The thermal insulation between the hot section and the water-cooled section was obtained by a boron nitride (BN) spacer that did not insulate as well as thought possible so it was replaced by

a pyrolytic graphite spacer. The graphite spacer was superior to the BN piece. The hot sections were made of molybdenum and later molybdenum with tungsten inserts in the constrictor region. The gas injector design is important to obtain proper mixing of the fuel and oxidizer. We chose to use a coaxial design sketched in Figure 8, where the fuel/oxidizer ratio determines the cross-sectional area ratio of the inner fuel to outer oxidizer. The oxidizer was fed in the outer two open “pie” sections to help keep the fuel cool until proper mixing in the combustion chamber can be achieved, thus preventing cracking of the acetylene. The arcjet was fabricated with two tangential injectors located at 180° apart and they were balanced by adjustable needle valves in one injector, one each for fuel and oxidizer.

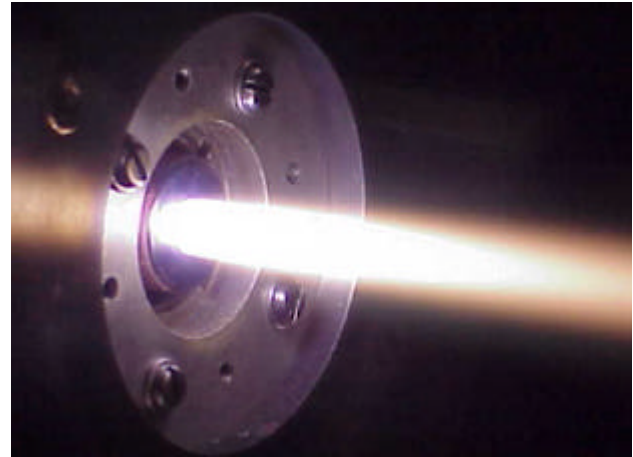
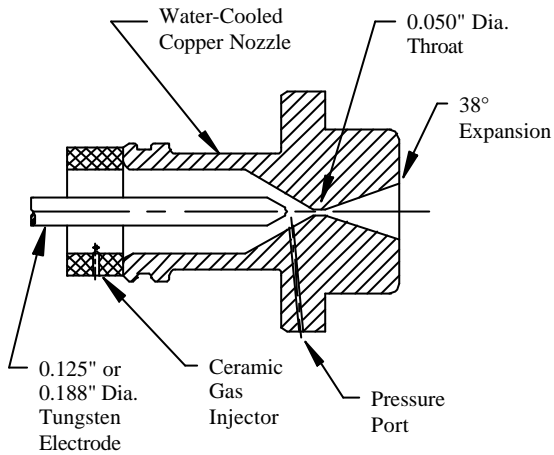


**Figure 4** Busek laboratory water-cooled arcjet. **Figure 5** Water-cooled arcjet, 3.5 kW, gas is (19%CO + 24%N<sub>2</sub> + 57%H<sub>2</sub>).

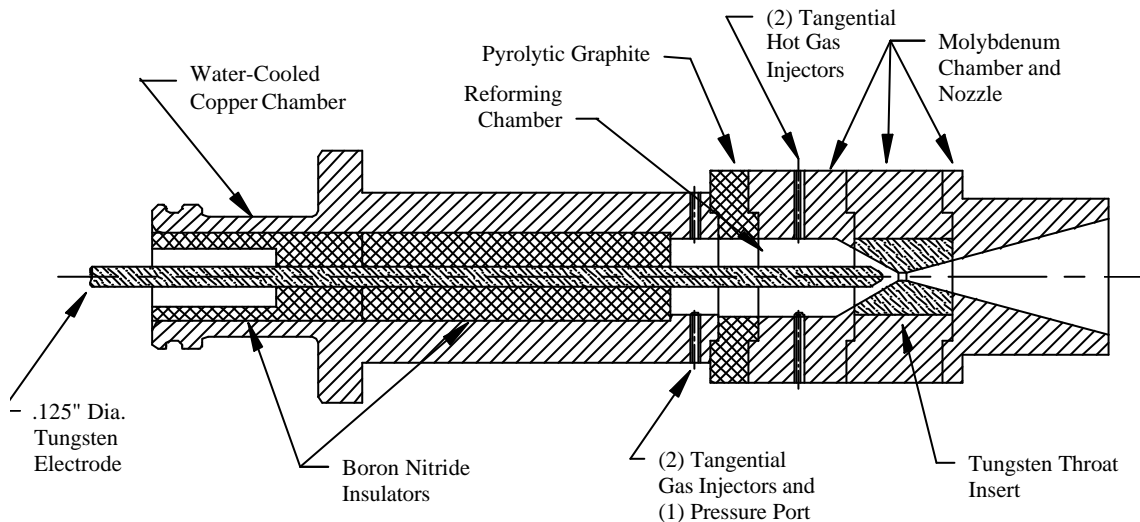


**Figure 6** Sketch of the bipropellant hybrid arcjet laboratory model

The typical operational steps for the hybrid arcjet involved preheating of the walls as follows: 1.) flow (19%CO + 24%N<sub>2</sub> + 57%H<sub>2</sub>) gas at preset value, 2.) apply DC voltage at constant current setting set prior, 3.) strike arc with HF starter, 4.) adjust current setting until at desired power, 5.) operate until chamber and nozzle are orange hot, 6.) simultaneously switch off (19%CO + 24%N<sub>2</sub> + 57%H<sub>2</sub>) and switch on (C<sub>2</sub>H<sub>2</sub> + 2N<sub>2</sub> + 5H<sub>2</sub>) + (O<sub>2</sub> + ½ N<sub>2</sub>), 7.) adjust current and flow while recording data. As discussed previously, a preheat of the arcjet was thought necessary to prevent carbon condensing onto the cold arcjet surfaces if the arcjet was started with the reforming gases. The constrictor diameter was varied from 1.27mm to 2.03mm for most experiments and 3.81mm to 6.35mm for low pressure test. Convergence angle of anode & cathode tip angle varied from 20° to 90° included angle, both had same angles for most trials. Anode to cathode gap setting ranged from 0.51mm to 2.03mm for most runs, some exceptions of over 2.54mm. Mass flow was

varied extensively and ranged from as low as 3slpm to 25slpm total flow. Typically, for a given geometric condition, several flow rates were tested. Power input ranged from as low as 1kW up to 6.5kW. For all cases, the current was set and the voltage was allowed to fluctuate. Fuel/oxidizer ratio ranged from slightly below reforming ratio (just enough oxidizer to form CO) to 50% over stoichiometric. Length of the reforming chamber ranged from under 25.4mm up to 100+mm and the diameter of the chamber ranged from 9.53mm to 15.9mm. The cathode diameter varied from 3.17mm to 9.53mm.

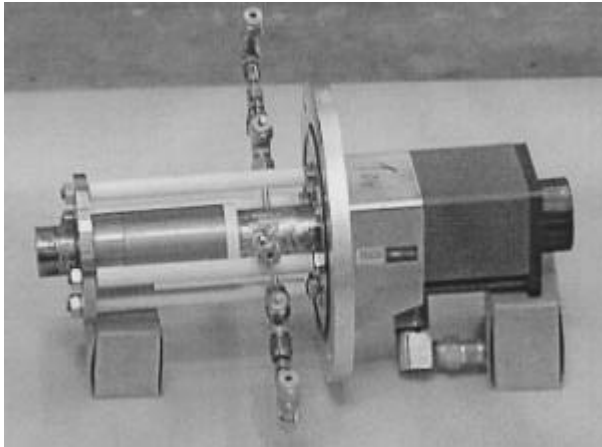


**Figure 7** Picture of one configuration of the laboratory hybrid bipropellant arcjet.

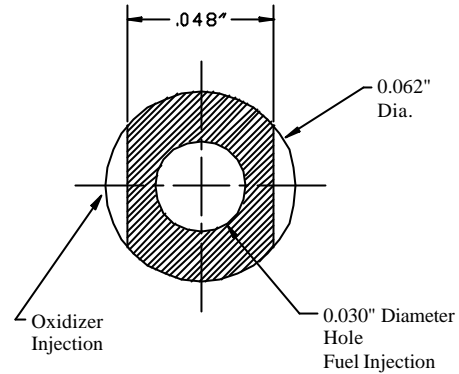


**Figure 8** Sketch of gas injector cross-section.

In all, over 200 experiments to improve the arcjet performance were conducted. Following is a condensed discussion on the experimental sequence. Some typical experimental data for acetylene mixture simulation is given in Table 2 and Figure 9 contains a picture of the arcjet nozzle and plume in simulated MMH/NTO reforming mode operation. Unfortunately, operation such as pictured only had run times of a few minutes maximum before carbon buildup in the throat ceased operation. The carbon precipitated out of the reforming reaction and deposited in the throat, on the expansion nozzle and exhausted in the jet plume. One example of the nozzle coated with soot and the throat plugged with hard carbon precipitate is shown in Figure 10.

**Table 2** Sample bipropellant arcjet experimental data for acetylene mixture simulation.

Voltage (volts)	Power (kW)	Flow (slpm)	Arc Pressure (Torr)	Throat Dia. (mm)	Results
91	2300	6	860	0.76	Carbon buildup, then throat melting.
80	4100	6	1100	1.27	"
78	3950	11	1020	1.52	Carbon buildup, throat gouged.
85	4770	15	1251	1.52	Carbon buildup.
84	4700	15	710	2.03	Carbon buildup, throat gouged.
84	3260	15	569	2.54	Carbon in the plume, nozzle.

The fuel gas mixture composition was changed from ethylene to acetylene containing early on in the project with little effects on arcjet operation. The throat region of the anode was switched from molybdenum to a tungsten insert due to throat melting. The tungsten did perform better, but carbon plugging still the major problem. The boron nitride insulator between the water-cooled section and the hot section was replaced by quartz then pyrolytic graphite to reduce thermal conduction. The pyrolytic graphite performed outstandingly. The gas injectors were moved to a hot region of the arcjet from the water-cooled section without any observable difference in arcjet performance.

A method to prevent carbon particulate formation was thought possible if the fuel/oxidizer ratio upstream of the arc, in the reforming region, was decreased so that the oxidizer was now above the reforming ratio. This excess oxygen lead to rapid anode and cathode oxidation and depletion. Gas shielding of the anode throat region with fuel gas was attempted by tangential injection just upstream of the throat with little to no success. The last attempt at gas shielding was normal reforming mode gas injection with additional tangential injection of excess oxidizer just before the throat. All attempts formed carbon unless the oxidizer was increased above stoichiometric percentages. At the high oxidizer flows, the throat and cathode oxidation

and vaporization were quick to follow. At this point, numerical simulations of the reforming process proved to be very enlightening.

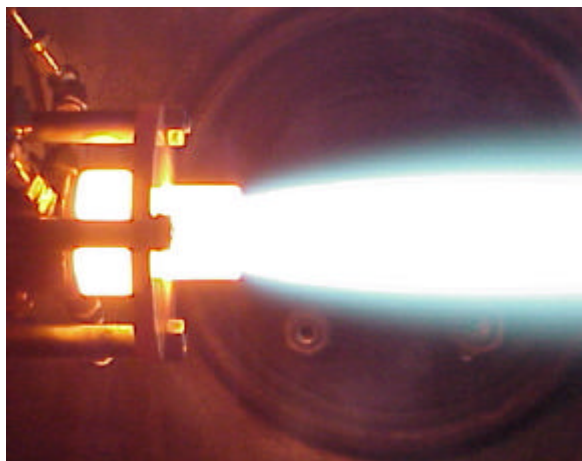


**Figure 9** Hybrid arcjet operating with simulated MMH/NTO.

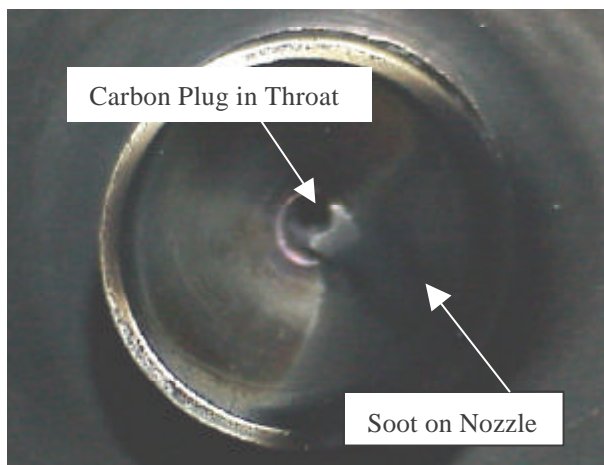


**Figure 10** Picture of nozzle looking upstream, showing hard carbon plug in throat and carbon soot particles on nozzle expansion wall.

### Numerical Chemical Kinetics

To better understand the reforming reaction within the reforming region of the arcjet, before the arc region, Aerodyne Research, Inc., performed chemical kinetic numerical simulations<sup>2</sup> using two kinetics codes. The PSR code<sup>3</sup> was used for most of the modeling work. This is a perfectly-stirred reactor model which solves the mass and energy balances for an ideal, perfectly-stirred reactor having user-specified values for the reactor residence time, reactor pressure, reactant inlet temperature, and reactor heat loss. Assuming the reactants in the actual hardware are well-mixed, PSR provides a good representation of the fuel reforming region in an arcjet. The standard output of PSR is the species distribution and temperature of products. Rates of production and consumption of selected species are an optional output. PSR was typically run for reactor residence times ranging from 1 ms to 10s. While PSR provides a good representation of a reaction region for reforming MMH or synthetic mixtures, it does not provide a time history of the reactions that take the initial reactants to final products. The CHEMKIN code<sup>4</sup> provides this time history, so it has been run for the MMH and synthetic mixtures to provide additional insight into the kinetics of the reformation process. The basic mechanism for MMH decomposition and reaction was taken from Catoire<sup>5</sup> with slight modifications. CHEMKIN is typically run at a specified temperature and pressure. The output is the distribution of species in the mixture as a function of time. The CHEMKIN calculations used an initial “kick” of 1% H atom mole fraction in the initial mixture to start the reaction process. The CHEMKIN results were determined to not be sensitive to moderate variations in this initial kick. The results from this study are summarized below.

A graph of the CHEMKIN results for the simulated MMH/NTO mixtures at 2000K and one atmosphere pressure is shown in Figure 11 (time in seconds) for the mole fractions of major carbon and oxygen containing species. Nitrogen was a non-contributor to the CO reaction and was excluded along with minor species and H<sub>2</sub>. Note that the oxygen reacts nearly instantaneously with hydrogen to form water vapor. The results indicate that carbon reformation to CO in synthetic mixtures occurs relatively slowly, primarily because H<sub>2</sub>O is the main oxidizing agent and H<sub>2</sub>O is a weak oxidizer. H<sub>2</sub>O mole fractions above 5% are present for **100ms**. Increasing the reactor temperatures improved the reforming process, though temperatures above 2300K would be needed to reduce the H<sub>2</sub>O mole fraction below 2% for a 50ms residence time. Similar results were obtained for PSR simulations as shown in Figure 12. The typical residence time for an arcjet is 5-10 ms maximum, more than an order of magnitude less than required. Ethylene fuel mixtures replacing acetylene mixtures were simulated with similar results.

The actual MMH + ½ NO<sub>2</sub> (for NTO) simulation results are shown for CHEMKIN and PSR in Figure 13 and Figure 14 respectively. The reaction time to CO is predicted to be more than an order of magnitude slower than for the simulated gases or more than two orders of magnitude longer than exists in the typical arcjet. These numerical simulations explained the insensitivity of our experimental results to operating conditions and wall geometry.

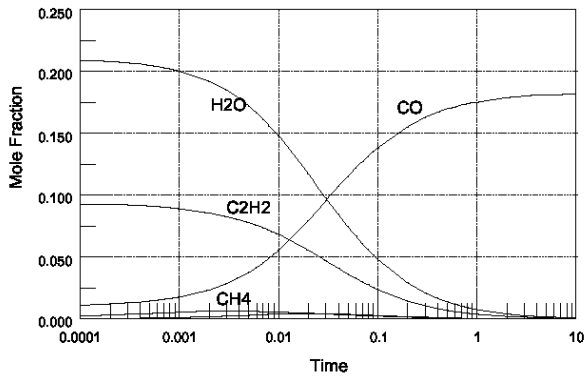


**Figure 11** CHEMKIN simulation for  $C_2H_2 + 2.5N_2 + 5H_2 + O_2$  reforming at 2000K & 1 atmosphere.

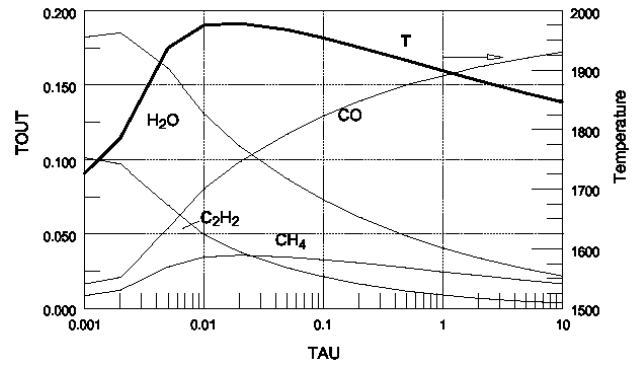


**Figure 12** PSR simulation output for  $C_2H_2 + 2.5N_2 + O_2 + 5H_2$  at 1 atmosphere.

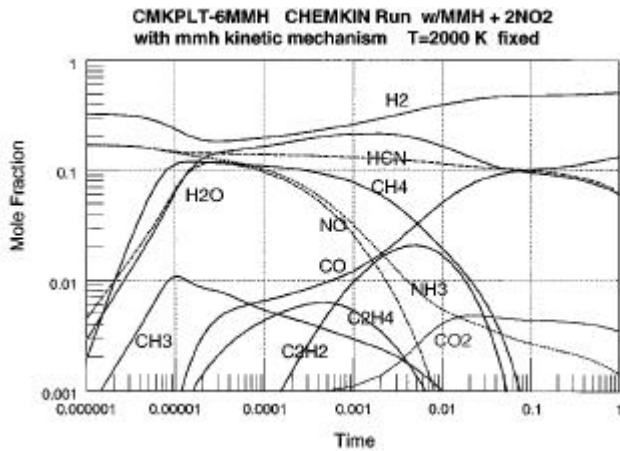


**Figure 13** CHEMKIN results for MMH + 0.5 NO<sub>2</sub> reactants at T=2000K & 1 atmosphere.

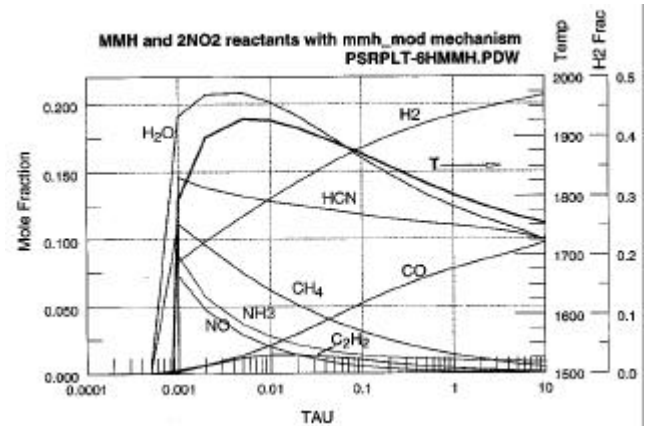


**Figure 14** PSR results for MMH + 0.5 NO<sub>2</sub> reactants at 1 atmosphere.

### RF “Arcjet” Development

Due to the unstable operation of the DC arcjet as a consequence of the carbon precipitation and subsequent throat/nozzle clogging or the material oxidation, an alternative bipropellant electric thruster configuration was sought. After an extensive exploration, we decided that an inductive RF thruster utilizing the complete stoichiometric combustion of MMH/NTO  $\{N_2H_3(CH_3) + 5/4 N_2O_4 \rightarrow 3H_2O + CO_2 + 9/4N_2\}$  would be the best option. This thruster would again utilize the chemical energy release of the bipropellants and then increase the enthalpy of this reacted gas by depositing energy via an RF inductive discharge. In an RF inductive discharge, the principle link between the RF power supply and the plasma is RF currents induced by transformer action in the plasma. The power can be delivered without the requirement for electrodes in contact with the plasma. This resolves all problems of electrode oxidation when operated at stoichiometric conditions. Another unique feature of this thruster is that it can be fueled at almost any fuel/oxidizer ratio and by almost any gas. Several iterations of the RF thruster design led to the quartz construction as sketched in Figure 15 named the “RF Arcjet”. In this figure, the gas is fed and mixed in a quartz tube that ends in a sudden expansion that is used as a flame holder, here the gas combusts, initiated by the RF. After combustion, the gas products pass through the inner region of the induction coil where via displaced currents, electrical energy is added to the electrons, which then transfer their energy to the gas as a whole.

The schematic of the RF circuit is shown in Figure 16, where  $L_c$  &  $R_c$  are the coil inductance and resistance respectively and  $L_g$  &  $R_g$  are the gas inductance and resistance respectively. The RF generator used was a Plasma Therm HFP-2500, 2.5kW, 27.12MHz, pentode tube based RF generator. The discharge was initiated by a 10-50kV Tesla coil. All coils were fabricated from copper tubing in two diameters, 1/8” & 1/4” and were water-cooled with forced ( $\approx 90$ psi) chilled water. Coils losses were measured to be about 35% as wound and were reduced to 20% or less by silver plating. Another approach to lower coil losses is to increase surface area, such as square tubing, though none were attempted to date.

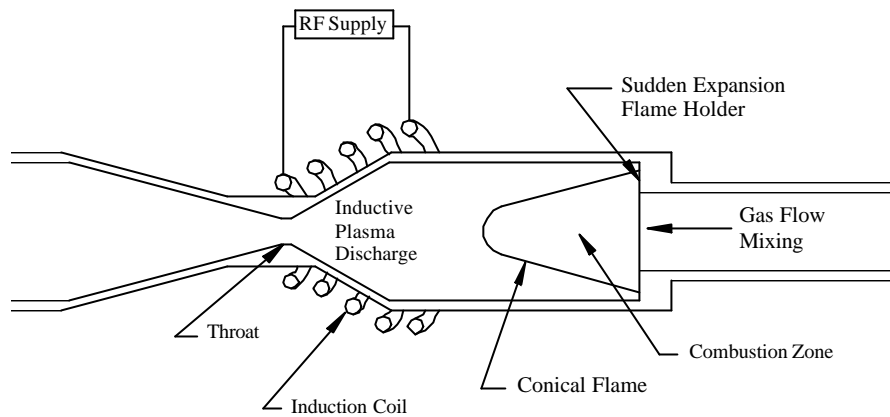


**Figure 15 Laboratory RF Arcjet with Combustion Upstream of the Inductive Discharge.**

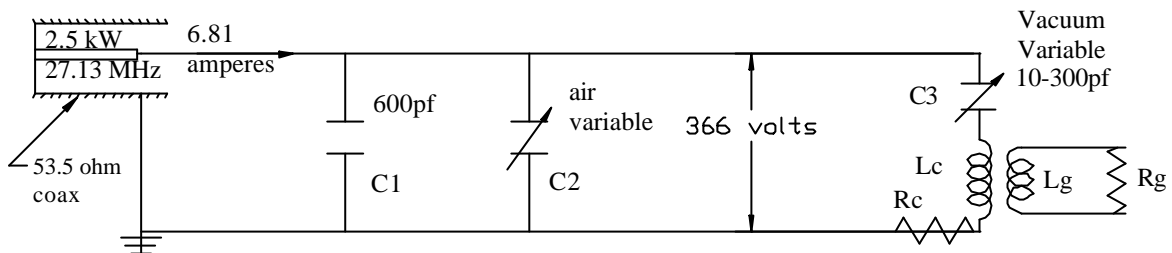


**Figure 16 Schematic of the RF circuit used in RF arcjet research.**

### RF Arcjet Experiments

The RF Arcjet experiments were very successful. Typical operation started with flowing small amounts of gas, either fuel or oxidizer or both, and powering the RF coil to low power. The discharge was initiated by a small high frequency Tesla coil. Once initiated, flow and power were increased and a combustion flame appeared in the wake of the flame holder as shown in Figure 17 and Figure 18. By shortening the combustion region and moving the coil near the throat as shown in Figure 18, some of the losses through the quartz were eliminated. Experimental data and estimated total  $I_{sp}$  are given in Table 3. The total  $I_{sp}$  is estimated by assuming that the  $I_{sp}$  is proportional to the square root of enthalpy, where  $I_{sp (Total)} = I_{sp (Chemical)} \times (h_{Total}/h_{Chemical})^{1/2}$ . The RF Arcjet can be operated on just about any gas including water vapor, hydrogen/oxygen, methane, air, etc. As an example, Table 4 shows the results for  $\text{GH}_2/\text{GO}_2$ .

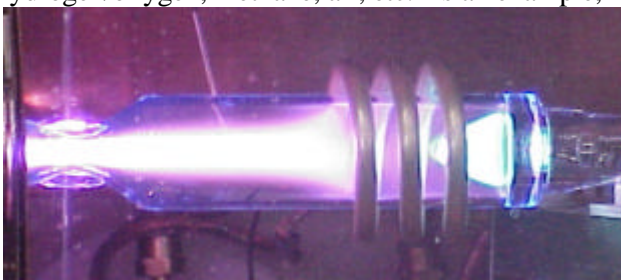


**Figure 17 Simulated MMH/NTO laboratory RF Arcjet, upstream coil.**



**Figure 18 Simulated MMH/NTO laboratory RF Arcjet, coil at throat.**

The technology concerns of an RF Arcjet are: 1.) coil losses, 2.) cooling of coil, 3.) cooling of quartz chamber, and 4.) RF generation technique and efficiencies. Coil losses have been narrowed to less than 20% by silver plating and with surface area addition, coil losses of 10% and under is entirely possible. With these losses down, heating of the coil will largely be from radiation from the discharge. We feel that regenerative cooling of a dielectric chamber will be required and cooling of the coil could also be regenerative. Rough calculations using water (l) suggest that regenerative cooling is possible, though with NTO more work needs to be done. Directed Energy, Inc. currently markets MOSFET technology in the kW range applicable for 13.56 MHz generation at 90% efficiency<sup>6</sup>.

**Table 3 Simulated MMH/NTO combustion plus RF induction heating data.**

RF Power Incident = 1950W	Chemical Enthalpy = 168 kJ/mole
RF Power into Gas = 1325W	RF Enthalpy input = 596kJ/mole
Fuel Flow = 2.00 slpm	Total Enthalpy = 764 kJ/mole
Oxidizer Flow = 2.40 slpm	Enthalpy Ratio Total/Chem. $\approx$ 4.54
Products Molecular Weight = 21.95	Chemical Isp $\approx$ 300s
Chamber Pressure = 42 Torr	Estimated Total Isp $\propto \sqrt{\text{enthalpy}}$ = <b>600s</b>

**Table 4 GH<sub>2</sub>/GO<sub>2</sub> combustion plus RF induction heating data.**

RF Power Incident = 1815W	Chemical Enthalpy = 241 kJ/mole
RF Power into Gas = 1232W	RF Enthalpy input = 807kJ/mole
Fuel Flow = 2.00 slpm	Total Enthalpy = 1048 kJ/mole
Oxidizer Flow = 1.0 slpm	Enthalpy Ratio Total/Chem. $\approx$ 4.35
Products Molecular Weight = 18.0	Chemical Isp $\approx$ 330s
Chamber Pressure = 50 Torr	Estimated Total Isp $\propto \sqrt{\text{enthalpy}}$ > <b>600s</b>

### Conclusions

We were unable to operate the DC bipropellant hybrid arcjet for extended periods of time with simulated MMH/NTO in reforming ratios without forming carbon particulates or oxidizing electrodes. The cathode shielding with additional oxidizer experiments have proven to be very difficult if possible at this scale size. CHEMKIN and PSR numerical simulations agree with experiments by showing that the acetylene or ethylene mixtures to simulate MMH plus NTO reforming reactions were slow, on the order of 100ms. Actual MMH/NTO reforming numerical simulations determined the propellant reforming reactions were even slower than our simulated propellants. The typical residence time of an arcjet is 5-10ms maximum. Therefore, it appears difficult if not impossible to operate a DC arcjet with MMH/NTO without carbon precipitation or electrode oxidation.

Our focus was redirected to an electric thruster where no plasma contact with the electrodes takes place, allowing the thruster to operate at stoichiometric conditions. An RF inductive discharge was selected and we designed and fabricated an RF Arcjet. This engine was a success with no carbon formation nor electrode oxidation for what appears to be unlimited run times. Burning the MMH/NTO at stoichiometry ratios and with the addition of RF energy, estimated specific impulses on the order of 600s were calculated. In addition, GH<sub>2</sub>/GO<sub>2</sub> propellant was utilized in a separate test with the same success. The RF Arcjet has what seems to be an unlimited schedule of propellant options. Technology concerns have been stated and possible means of solving them initiated.

As noted in Table 3 and Table 4, the chamber pressure is of the order of several tens of Torr with 100 Torr achievable. This is a very high pressure for conventional RF discharges and very low pressure relative to the conventional low thrust chemical engines that operate at three orders of magnitude higher pressure. The preheating of the plasma gas by combustion upstream of the RF discharge zone allows the RF discharge to exist at the relatively high pressure and mitigates possible nonequilibrium ionization as well as significant dissociation, both of which could lead to lower engine efficiency. The very attractive consequence of this discharge pressure are the low heat and structural loads on the RF Arcjet components which can be then be made of simple oxides with indefinite life. By contrast, the low thrust chemical engines require expensive advanced alloys and/or precious metals and can not operate at conditions other than fuel rich.

### Acknowledgement

This research is supported by a NASA Phase II SBIR contract. We acknowledge gratefully the support given by Dr. M. Domonkos, the NASA Glenn technical monitor of this contract.

- 1 Hruby, V., et al., "Methane Arcjet Development", IECP 97-014, 25<sup>th</sup> International Electric Propulsion Conference, Cleveland, OH, August 1997.
- 2 Annen, K. and Brown, R., "Modeling of Carbon Reforming Processes For MMH Arcjet Experiments", ARI-RR-1327, December, 2001.
- 3 Glarborg, P., Kee, R.J., Grcar, J.F., and Miller, J.A., PSR: A Fortran Program for Modeling Well-Stirred Reactors, Sandia Report SAND86-8290, Sandia National Laboratories, 1992.
- 4 Kee, R.J., Miller, J.A., and Jefferson, T.H., CHEMKIN, SAND80-8003 (1980).
- 5 Catoire, L., et al., "Ignition Delays in MMH+CH<sub>4</sub>+O<sub>2</sub>+Ar Mixtures", J. Propulsion and Power 17, 1085, 2001.
- 6 Directed Energy, Inc. Technical Note, "PRF-1150 1kW 13.56 MHz Class E RF Generator Evaluation Module", 2002.